water

MDPI

Article

Analyzing the Akinete Protein of the Harmful Freshwater Cyanobacterium, *Dolichospermum circinale*

Keonhee Kim [1], Chae-Hong Park [1] and Soon-Jin Hwang [1,2,*]

[1] Human and Eco-Care Center, Department of Environmental Health Science, Konkuk University, Seoul 05029, Republic of Korea; skyopera@konkuk.ac.kr (K.K.); qkrcoghd@konkuk.ac.kr (C.-H.P.)
[2] Department of Environmental Health Science, Konkuk University, Seoul 05029, Republic of Korea
* Correspondence: sjhwang@konkuk.ac.kr; Tel.: +82-2-450-3748

Abstract: Akinete is a survival structure in cyanobacteria that has overcome unfavorable environmental conditions and influences their perennial blooms in the freshwater system. However, the akinete cellular and biochemical properties are insufficiently explored. We analyzed the akinete structure, as well as akinete-specific proteins and their amino acid sequence. Akinetes of *Dolichospermum circinale* were produced from their vegetative cells isolated from the North Han River, Korea. The akinete protein was obtained using electrophoresis, and utilizing its amino acid sequences, its antibody-binding reaction potential (ig-score) was quantified. Akinete protein masses were 17 kDa–180 kDa, and the akinete protein mass was 110 kDa. The ig score was high (average 5.0121 points) in the first half of the amino acid sequence, indicating a β-turn form. The amino acid sequence, having over 50% homology with the *D. circinale* akinete protein, was not present in GenBank. The homology of the *D. circinale* akinete-specific protein was very low (9.8%) compared to that of *Anabaena variabilis*, indicating that its composition was substantially different, even among phylogenetically close taxa. To the best of our knowledge, this is the first report on the *D. circinale* akinete protein and its amino acid sequence, with preliminary information for their practical application for detecting akinetes in freshwater systems.

Keywords: cyanobacteria; akinete; protein; amino acid; antibody; *Dolichospermum circinale*; North Han River

check for updates

Citation: Kim, K.; Park, C.-H.; Hwang, S.-J. Analyzing the Akinete Protein of the Harmful Freshwater Cyanobacterium, *Dolichospermum circinale*. *Water* **2023**, *15*, 2746. https://doi.org/10.3390/w15152746

Academic Editors: Eva Papastergiadou and Kostas Stefanidis

Received: 6 July 2023
Revised: 24 July 2023
Accepted: 27 July 2023
Published: 29 July 2023

1. Introduction

Cyanobacteria from the orders of Nostocales and Stigonematales form akinetes as a survival structure [1]. Akinetes located in the sediment can survive in adverse environmental conditions for a long period; when conditions become favorable, they germinate to develop vegetative cells that could proliferate in the water layers [2–4]. Some filamentous cyanobacteria forming akinete, such as *Dolichospermum*, *Aphanizomenon*, and *Cylindrospermopsis*, are known to be harmful because they cause blooms and produce odorous materials and toxins, thereby causing negative effects on water use and ecosystem health [4–7]. Therefore, information on the spatiotemporal distribution of akinetes in the sediment and factors affecting akinete germination provides important evidence for early warnings in water management, since they can serve as one of the precursors to cyanobacterial blooms in the area [8,9].

Akinete detection in situ has some constraints because it is located in the sediment. Analyzing ambient distribution and the abundance of akinetes requires their separation directly from the sediment, followed by their microscopic observation [10–12]. In the conventional method dealing with akinetes from sediment samples, cells are separated individually using micropipettes after ultra-sonication and serial size fractionation [13]. However, it is difficult to completely remove soil particles and organic materials attached to akinetes, preventing the complete separation of the akinete from the sediment. The efficiency of the various separation methods varies; therefore, the need for an effective detection method has been increasingly recognized [14–16].

Molecular-level detection techniques, which are based on DNA and mRNA, could overcome the limitations of the physical separation methods [17–19], because they utilize the whole sediment without an akinete separation process. Several studies have been conducted on cyanobacteria that possess genes producing harmful material, using molecular detection to overcome the limitations of microscopic analysis [20–22]. Similarly, in the field of akinete monitoring, molecular techniques would be more useful to detect akinete cells in the sediment [23]. However, there are limitations to molecular detection on the gene level. With DNA-based methods, it is difficult to either selectively amplify or stain the DNA of akinete cells as demonstrated in the PCR and CARD-FISH (catalyzed reporter deposition–fluorescence in situ hybridization) methods; therefore, it is difficult to verify actual akinete production. Furthermore, there is a time limit of the mRNA-based method for detecting akinete in situ, because mRNA can only be detected for a short period when the akinetes are formed.

The akinete protein persists for a prolonged period in the sediment environment, because the akinete possesses a thick cell wall. In addition, the protein degrades more slowly than mRNA after synthesis. Therefore, if the akinete protein is applied, the limitation of the short detection period that occurs at the mRNA level can be overcome. To date, however, there are limited studies on akinete proteins and the amino acid sequences. Information on the akinete protein and its amino acid sequence for only *Anabaena variabilis* and *Anabaena cylindrica* are available in the global amino acid database (NCBI: National Center for Biotechnology Information) [24–26]. Currently, there is no information regarding the akinete protein of *Dolichospermum circinale*, which frequently causes blooms and produces toxins and geosmin in eutrophic freshwater systems [27].

The purpose of this study was to elucidate the akinete-specific protein and the amino acid sequence of the harmful cyanobacterium, *D. circinale*. The result will be an important addition to akinete protein research and provide preliminary information for developing akinete detection methods.

2. Materials and Methods

2.1. D. circinale Isolation and Culture

Vegetative cells of *D. circinale* were collected from the downstream area of the North Han River (37°35′16.72″, 127°20′25.23″) in August 2015, during its bloom. They were stored in a cool icebox immediately after collection and transported to the laboratory within 5 h. The filaments of *D. circinale* were separated into a single strand using the capillary method [28], and the single strand was inoculated on a 96-well plate (Falcon®, Newark, NY, USA) containing the BG-11 medium (Merck Co., Darmstadt, Germany) [29]. Thereafter, the cells were cultured for 30 d in an incubator (VS-8480, Vision, Daejeon, Republic of Korea) at 25 °C and a light intensity of 130 $\mu E/m^2/s$ (14:10 = L:D). A healthy strain showing good growth in the well plate was selected and transferred into a flask with 100 mL BG-11 medium (Merck Co.), and the culture was grown until it reached the log phase.

Akinetes from natural samples to be used for analyzing morphological characteristics were collected from a surface layer of the sediment. The sediment sample was collected using a core sampler (Uwitec, Mondsee, Austria) at the same place as the sampled vegetative cells. The collected sediment sample was then transferred to the laboratory, and 1 g (*w*/*w*) was suspended in sterilized water. The suspension was treated twice with ultrasound for 20 s using an ultrasonic device (JAC 4020 type, 60 Hz, 620 w, Ultrasonic, Hwasung-si, Republic of Korea). The pulverized suspension was sequentially filtered through 100, 60, and 10 μm nylon mesh to isolate akinetes. Following the panning method [13], the filtrate was placed on a petri dish (12 cm in diameter), and from the top layer, the floating particles were isolated and mixed with filtered (0.2 μm) sterile water to a final volume of 10 mL. The final solution was stored in a dark brown glass bottle at approximately 4 °C.

2.2. Akinete Preparation

A laboratory designed culture chamber was used to induce akinete formation from *D. circinale* vegetative cells. The chamber could be operated such that the upper and lower parts were separate to simulate the water layer and the sediment, respectively [30]. *D. circinale* vegetative cells were inoculated at a density of 5×10^4 cells/mL in the upper cylinder filled with BG-11 medium. Artificial sediment [31] formulated in the laboratory was placed in the lower cylinder. The chamber, equipped with both the upper and lower cylinders, was placed in an incubator at 20 °C and a light intensity of 30 $\mu E/m^2/s$ (14:10 = L:D) for 5 d to induce akinetes [30]. Akinetes were collected from the sediment of the lower cylinder in the chamber, concentrated using a 10 μm sieve in 10 mL of distilled water, and stored in a dark brown glass bottle under refrigeration at 4 °C.

Subsequently, 1 mL of the refrigerated sample was placed in a Sedgwick–Rafter chamber and the morphological features [32,33] of the akinetes were observed at 400× magnification on an inverted microscope (Axiovert A1, Zeiss, Oberkochen, Germany) (Figure S1). The akinetes were separated individually using a microcapillary [34]. The external morphology of the separated akinetes was examined using an optical microscope (Axio Scope A1, Zeiss) and scanning electron microscope (JSM-7500, Jeol, Akishima, Japan).

2.3. Protein Extraction from Akinete and Vegetative Cell

D. circinale akinetes and vegetative cells were transferred to different microtubes and centrifuged at 20,000 rpm (6708× *g*) for 30 min. The supernatant of each sample was removed and lysis buffer (50 mM Tris-HCl pH 8.0, 150 mM NaCl, 5 mM EDTA,1% NP-40, and protease inhibitor cocktail) was added and left to react for 5 min on ice to facilitate cell lysis. The intracellular substances of the reacted samples were eluted with ultrasound homogenizers (VCX500, Sonics & Materials, Inc., Newtown, CT, USA). The soluble protein present in the supernatant was separated using centrifugation at 4 °C and 13,000 rpm (2834× *g*) for 10 min. Separated proteins were analyzed using the Bradford assay [35]. A 4 × SDS (sodium dodecyl sulfate) sample buffer (#161-0747, Bio-Rad laboratories, Portland, OR, USA) was added to the protein sample. It was then heated to 100 °C for 5 min to obtain a primary protein structure with a negative charge (i.e., a linear shape). Markers were loaded on 12% acrylamide SDS-Poly Acrylamide Gel Electrophoresis (PAGE) gels. Electrophoresis on SDS-PAGE gel was performed at 120 V for 2 h to separate the proteins based on their mass. SDS-PAGE gels were stained with Coomassie Brilliant Blue R-250 solution (Sigma, St. Louis, MO, USA) for more than 24 h and then a destaining solution (10% acetic acid and 45% methanol in 1 L distilled water (DW)) was applied for 1.5 h to remove the background color to obtain protein bands. Protein bands exclusively present in the akinete samples were selected for further analysis.

2.4. Sample Preparation for Mass Spectrometry

Akinete-specific protein bands were cut out from SDS-PAGE gel using a scalpel and transferred to sterilized microtubes. Then, the peptide bonds between amino acids were degraded using an in-gel digestion reaction (in-gel trypsin degradation) [36].

Excised gel spots were destained with 100 μL of destain solution (50% Acetonitrile (ACN)/DW) with shaking for 5 min. After the removal of the solution, gel spots were incubated with 200 mM ammonium bicarbonate (NH_4HCO_3) for 20 min. The gel pieces were dehydrated with 100 μL of ACN and dried in a vacuum centrifuge (VS-30000i, GSI, Republic of Korea). Into the dried gel piece, 50 μL dithiothreitol (10 mM) mixed with 0.1 M ammonium bicarbonate was added and this was incubated at 56 °C for 30 min with shaking. The sample was spun down and the supernatant was removed. Subsequently, 100 μL ACN was added for gel shrinkage. Fifty microliters of iodoacetamide (C_2H_4INO) (55 mM) mixed with 0.1 M ammonium bicarbonate was added and incubated at room temperature for 20 min in the dark. The supernatant was removed and 200 μL ACN was added. Again, it was spun down to remove supernatant, and 200 μL ammonium bicarbonate (0.1 M) was added. The procedure was repeated thrice on the dried gel piece. The dried gel pieces were

rehydrated with 20 μL of 50 mM NH_4HCO_3 containing 0.2 g modified trypsin (Promega Co., Madison, WS, USA) for 45 min on ice. After the removal of the solution, 30 μL of 50 mM NH_4HCO_3 was added. The digestion was performed overnight (6–8 h) at 37 °C. The peptide solution was desalted using C18 column (Ziptip, Millipore Co., Burlington, MA, USA). All processed protein samples were analyzed using MALDI-TOF (matrix-assisted laser desorption ionization time of flight) [37] and a protein sequencer (ABI494, Thermo Fisher Scientific, Waltham, MA, USA) (Table S1).

2.5. Analysis of Amino Acid Sequence

The sequenced amino acid was identified by protein BLAST analysis in the Genbank database. The BLAST searching was performed based on the Protein Data Bank proteins (PBD) in Genbank standard database, using the Protein–Protein BLAST (BLASTP) algorithm. We excluded the uncultured/environmental sample sequence, that is, unidentified sequence information, in the search process [38–40]. The hydrophobicity of the amino acid sequence (Kyte–Doolittle hydrophathy) and the immunogenicity score (ig-score) were analyzed based on predicted amino acid secondary structure [41]. The structure was predicted based on Chou–Fasman secondary structure model.

2.6. Statistical Analyses

In the akinete-specific protein amino acid sequence, the correlation between the ig-score and Kyte–Doolittle hydropathy of each section was analyzed to determine the relationship between protein hydrophobicity and antigen–antibody reaction potential. Pearson's correlation analysis was performed using SPSS version 18 (IBM, Armonk, NY, USA). Statistical significance was set at $p < 0.05$.

3. Results and Discussion

3.1. Protein Profile of D. circinale

The masses of proteins extracted from akinete ranged from 17 to 180 kDa. Proteins with masses in the range of 40–75 kDa were found in both the akinete and vegetative cells and comprised the largest portions of proteins present (Figure 1). They are speculated to comprise amino acids present in the plasma membranes, carboxysomes, polyphosphates, and cyanophycin granules; these organelles are present both in akinetes and in vegetative cells [42–44]. Small (30–48 kDa) and large proteins (180 kDa) were almost exclusively present in the vegetative cells. Physiologically active enzymes that are formed by various cellular organelles are normally present in active vegetative cells. These active enzymes are known to be very small (<48 kDa) [45–47]. Contrastingly, a miniscule amount of 30 kDa protein was present in akinetes. The 110 kDa protein was solely present in the akinetes (Figure 1). We did not identify whether this protein exclusively originated from the akinete cell wall or within the cell. However, because only the position of the 110 kDa protein showed no band in the extracts of vegetative cells, we considered it a candidate akinete-specific protein [48].

The akinete-specific proteins appear to differ even among similar taxa. The mass of the akinete-specific protein of *D. circinale* was 110 kDa, whereas that of the AvaK protein found in *Anabaena variabilis* akinete was 43 kDa [48]. A kind of akinete-specific protein, AcaK43, which is the AvaK homolog protein, was also found in *A. cylindrica* [49]. Therefore, we suspect that *D. circinale* has an akinete-specific protein, which is different from the AvaK protein in *A. variabilis* and the AcaK43 protein in *A. cylindrica*.

Consequently, the akinete-specific protein mass and peptide may affect the formation of akinetes, resulting in morphological and functional differences in the akinetes of the order Nostocales [50,51]. Morphologically, Nostocale taxa show different akinete shapes. The akinete of *D. circinale* is longer and wider than that of *A. variabilis* by approximately 10 μm (5–10 μm in length and 10–15 μm in width), and the length is similar in *A. cylindrica* akinete, but this is broader in width (length 15–20 μm and width 7–10 μm) (Figure S1). The projections present at both sides of the akinete anodes were present solely in *D. circinale*,

and not in *A. variabilis* or *A. cylindrica* [48,52]. Although photosynthesis is functionally not activated in akinetes, *A. cylindrica* showed photosynthetic proteins in both akinete and vegetative cells. However, in akinetes of *A. variabilis*, chlorophyll and phycocyanin disappeared during akinete cell maturation [53].

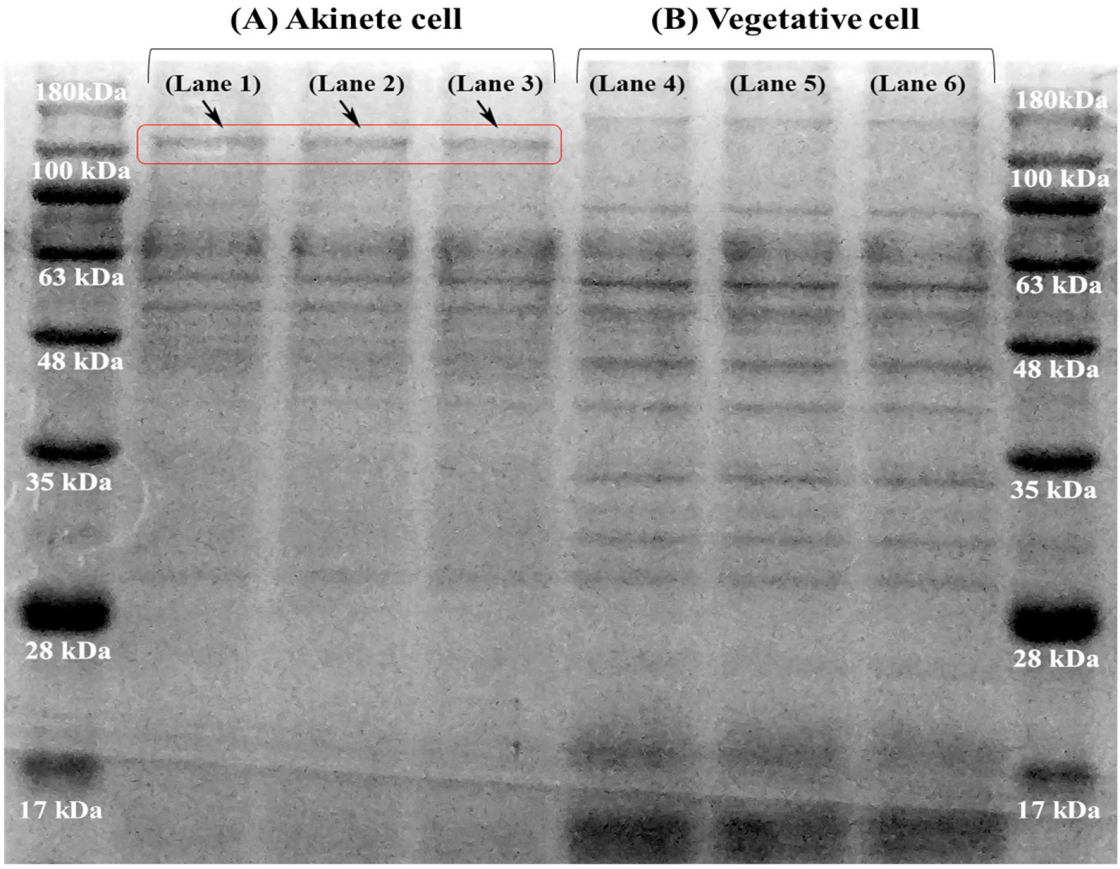

Figure 1. Bands of *Dolichospermum circinale* akinete and vegetative cell proteins displayed on SDS-PAGE gels (12%) stained using Coomassie Brilliant Blue R-250. The sample was loaded in triplicate. Vertically arrayed numbers in both the first and the last lane are the masses of standards in KDa. The arrows and square box indicate potential akinete-specific proteins. (**A**) Total cell protein extracted from akinetes (lane 1, 2, 3). (**B**) Total cell protein extracted from vegetative cells (lane 4, 5, 6).

3.2. Amino Acid Sequence of D. circinale Akinete-Specific Protein

We identified a peptide consisting of 600 amino acid sequences using the peptide mass fingerprint by MALDI-TOF, with the 110 kDa protein solely present in the akinete of *D. circinale*, as inferred from from SDS-PAGE bands (Table 1). The Chou–Fasman secondary structure and Kyte–Doolittle hydropathy index were determined using the peptide amino acid structure. Consequently, the ig-score, which indicates the antibody-binding reaction with the akinete-specific protein, was established (Figure 2, Table S3). The higher the ig-score, the higher the probability of the antibody initiating an immune response with the antigen [15]. The ig-score was higher in the No. 100–200 amino acid group and lower in the No. 470–600 amino acid group (Figure 2). The average ig-score of the whole amino acid sequence was 4.7745 (range: 2.3157–8.1835), whereas its average was 5.4254 between 105 aa and 210 aa. Specifically, the average score was the highest (avg. 6.4564) in the 110 aa–150 aa range. Moreover, the ig-score was high in the 273–345 aa (avg. 5.0602) and 405–475 aa ranges (avg. 5.0121). These results indicate that the amino acid sequence of the 105–349 aa range, particularly the 110–150 aa range, is better for detecting the akinete of *D. circinale*. Contrastingly, the ig-scores of the 5–112 aa, 220–270 aa, and 479–600 aa ranges

were lower than the average score. This suggests that the biosensing function (antibody) of the 220–270 aa amino acid sequence range might be relatively low.

Table 1. Amino acid sequence of the *D. circinale* akinete-specific protein analyzed from the 110 kDa sodium dodecyl sulfate poly acrylamide gel electrophoresis (SDS-PAGE) band.

No.	Amino Acid Sequence	No.
1	MKWVTFISLL LLFSSAYSRG VFRRDTHKSE IAHRFKDLGE EHFKGLVLIA	50
51	FSQYLQQCPF DEHVKLVNEL TEFAKTCVAD ESHAGCEKSL HTLFGDELCK	100
101	VASLRETYGD MADCCEKQEP ERNECFLSHK DDSPDLPKLK PDPNTLCDEF	150
151	KADEKKFWGK YLYEIARRHP YFYAPELLYY ANKYNGVFQE CCQAEDKGAC	200
201	LLPKIETMRE KVLASSARQR LRCASIQKFG ERALKAWSVA RLSQKFPKAE	250
251	FVEVTKLVTD LTKVHKECCH GDLLECADDR ADLAKYICDN QDTISSKLKE	300
301	CCDKPLLEKS HCIAEVEKDA IPENLPPLTA DFAEDKDVCK NYQEAKDAFL	350
351	GSFLYEYSRR HPEYAVSVLL RLAKEYEATL EECCAKDDPH ACYSTVFDKL	400
401	KHLVDEPQNL IKQNCDQFEK LGEYGFQNAL IVRYTRKVPQ VSTPTLVEVS	450
451	RSLGKVGTRC CTKPESERMP CTEDYLSLIL NRLCVLHEKT PVSEKVTKCC	500
501	TESLVNRRPC FSALTPDETY VPKAFDEKLF TFHADICTLP DTEKQIKKQT	550
551	ALVELLKHKP KATEEQLKTV MENFVAFVDK CCAADDKEAC FAVEGPKLVV	600

Note: A—alanine, G—glycine, I—isoleucine, L—leucine, P—proline, V—valine, F—phenylalanine, W—tryptophan, Y—tyrosine, D—aspartic acid, E—glutamic acid, R—arginine, H—histidine, K—lysine, S—serine, T—threonine, C—cysteine, M—methionine, N—asparagine, Q—glutamine.

The hydropathy index (Kyte–Doolittle index) of the amino acid sequence, indicating the degree of hydrophobicity [41], shows a significant negative correlation with the ig-score ($r = -0.914$, $p < 0.01$, $n = 593$) (Table S2). This result suggests that antibody binding occurs more easily in the hydrophilic region outside the cell membrane than in the hydrophobic region inside the cell membrane. Therefore, biosensing for akinete detection could be more effective in the hydrophilic condition than in the hydrophobic condition.

While verifying the protein ID of the akinete-specific protein analyzed in this study, we found that the NCBI BLASTP Database (GenBank CDS) did not contain data consistent with the protein amino acid sequence of *D. circinale* akinete. However, when compared to the akinete-specific protein of *A. variabilis*, which is the only one known thus far [48], homology was very low (9.8%). Prior studies were conducted on the endospore of the *Bacillus* species, such as *Bacillus subtilis* and *Bacillus cereus* [54–58]. The protein information of these endogenous spores is composed of short fragments, smaller than 200 aa, and this endospore protein has very low homology (<1%) with the akinete-specific protein found in this study. Both the cyanobacterial akinete and bacterial endogenous spores are formed to overcome harsh conditions and are functionally the same. However, recent proteomic data indicate that, on the contrary to the results of conventional research, akinetes may also play an active role during filamentous growth. Specifically, the akinete was reported to play a role in the fixation of nitrogen and as a carbon storage transfer unit in filaments of

A. cylindrica [49]. Qiu et al. (2020) demonstrated that fixed carbon entered into akinetes from vegetative cells and was converted to glycogen by glycogen synthase, or into trehalose for osmoprotectant during the survival stage [49]. Although both the cyanobacterial akinete and bacterial endogenous spores are functionally the same, they exhibit different degrees of high heat and dry resistance, and different structures at the anatomical level of the cell, such as the cortex components surrounding the spores [58].

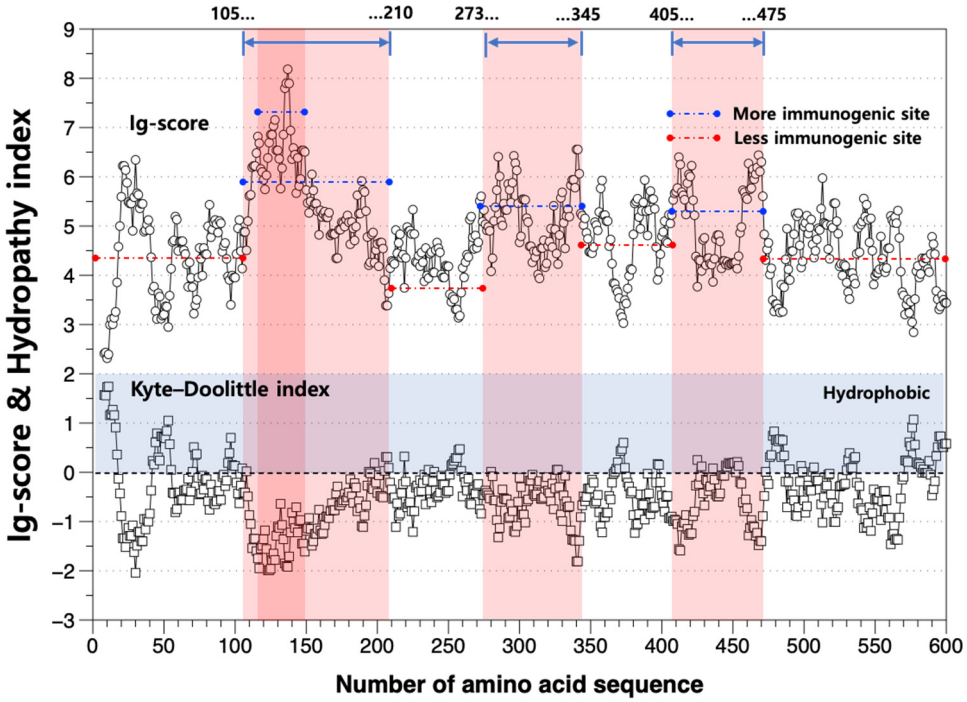

Figure 2. Immunogenicity score (ig-score) and hydropathy index of amino acid sequence of akinete-specific protein. Blue and red dashed lines indicate higher and lower score than the average score, respectively. The more immunogenic site was colored pink. In the hydropathy index graph, the parts that consist of positive values refer to the hydrophobic site.

3.3. Perspective on Developing the Akinete Screening Technique

The molecular-level approach has advanced harmful cyanobacterial detection in the field by using specific genes related with harmful material production [20–22]. However, molecular-level applications to identify akinetes exhibit some technical limitations because the akinete cell is surrounded by protein capsule. For this reason, proteomics research could help us to develop a method for the efficient screening of akinetes, such as an antibody biosensor or akinete-specific staining. However, there are some challenging technical hurdles from the practical perspective.

Firstly, it is difficult to verify actual akinete protein binding using the antibody based on the amino acid sequence analyzed in this study, because the best method for making the akinete-specific protein antibody is yet to be established [59]. Therefore, a further study to make an antibody against the akinete protein for screening cyanobacterial akinetes using the antigen–antibody reaction in field samples has high priority.

Secondly, it is necessary to develop a method for removing various non-specific protein polymers or organic particles remaining in the sediment to increase the sensitivity of the reaction with the akinete protein. In environmental proteins, which relate to similar concepts to environmental DNA, bulk proteins could include many non-specific protein polymers and organic particles [60]. They can disturb the activation of akinete-specific antibodies. For this reason, we must focus on establishing a sample purifying method for precise activation of akinete-specific antibodies.

Thirdly, due to the currently very limited information on the akinete protein and peptide, it is necessary to store akinete-specific protein peptide information from the Nostocales taxa [61,62]. Most cyanobacterial proteomics research has been focused on protein interaction networks that govern the lifecycle of cyanobacteria, such as post-translational mechanisms [63,64]. However, since 2002, there has been limited research on akinete-specific proteins. Further studies should include work on akinete peptides using various species from the order of Nostocales to expand our understanding of the species-specific akinete proteins and their role in physiology, and expedite the progress of cyanobacterial proteomics research.

4. Conclusions

D. circinale is the harmful cyanobacterium commonly found in eutrophic freshwater ecosystems. It forms akinetes as a survival structure. In this study, we analyzed the *D. circinale* akinete-specific protein and its amino acid sequence. To the best of our knowledge, the akinete-specific amino acid sequence of the order Nostocales determined in this study is only the third report on this topic, after those on *A. variabilis* and *A. cylindrica.* Although these species have very close phylogenic relationships, their akinete proteins differ in mass and have very low homology, suggesting that the akinete proteins are taxon-specific. Further studies are necessary to accumulate information on akinete proteins and their amino acid sequences among akinete-forming cyanobacteria, in order to establish a biosensing method based on antigen–antibody reactions. However, several technical hurdles need to be overcome related to the protein-level screening of akinetes for application in the field. Therefore, future research on akinetes in cyanobacteria must go beyond simple physiological studies and involve in-depth investigations at the metaomics level, which address the technical limitations at the protein level.

Supplementary Materials: The following supporting information can be downloaded at: https://www.mdpi.com/article/10.3390/w15152746/s1, Figure S1: Images of *D. circinale* akinete, Table S1: Analytical conditions of MALDI-TOF. Table S2: Result of the correlation analysis between the ig score and Kyte–Doolittle hydropathy index value. Table S3: Chou–Fasman secondary structure prediction for calculating ig score of *D. circinale*'s akinete-specific protein.

Author Contributions: Conceptualization, S.-J.H. and K.K.; methodology, K.K. and C.-H.P.; software, K.K.; validation, S.-J.H. and K.K.; formal analysis, K.K. and C.-H.P.; data curation, S.-J.H., K.K. and C.-H.P.; writing—original draft preparation, K.K.; writing—review and editing, S.-J.H.; supervision, S.-J.H. All authors have read and agreed to the published version of the manuscript.

Funding: This research was funded by Konkuk university in 2020 (2020-A019-0197).

Informed Consent Statement: Not applicable.

Data Availability Statement: The data used and analyzed during this study are available from the corresponding author on reasonable request.

Acknowledgments: The authors are very grateful to late Tae-Hyun Youm who helped with the protein extraction experiment.

Conflicts of Interest: The authors declare no conflict of interest.

References

1. Suikkanen, S.; Kaartokallio, H.; Hällfors, S.; Huttunen, M.; Laamanen, M. Life cycle strategies of bloom-forming, filamentous cyanobacteria in the Baltic Sea. *Deep Sea Res. Part II Top* **2010**, *57*, 199–209. [CrossRef]
2. Anderson, D.M.; Wall, D. Potential importance of benthic cysts of Gonyaulax tamarensis and G. excavata in initiating toxic dinoflagellate blooms 1, 2, 3. *J. Phycol.* **1978**, *14*, 224–234. [CrossRef]
3. Andersen, D.M.; Keafer, B.A. An endogenous annual clock in the toxic marine dinoflagellate Gonyaulax tamarensis. *Nature* **1987**, *325*, 616. [CrossRef]
4. Baker, P.D.; Bellifemine, D. Environmental influences on akinete germination of *Anabaena circinalis* and implications for management of cyanobacterial blooms. *Hydrobiologia* **2000**, *427*, 65–73. [CrossRef]

5. Huber, A.L. Factors affecting the germination of akinetes of *Nodularia spumigena* (Cyanobacteriaceae). *Appl. Environ. Microbiol.* **1985**, *49*, 73–78. [CrossRef]
6. Ståhl-Delbanco, A.; Hansson, L.-A. Effects of bioturbation on recruitment of algal cells from the "seed bank" of lake sediments. *Limnol. Oceanogr.* **2002**, *47*, 1836–1843. [CrossRef]
7. van Dok, W.; Hart, B.T. Akinete germination in *Anabaena circinalis* (cyanophta). *J. Phycol.* **1997**, *33*, 12–17.
8. Anderson, D.M.; Glibert, P.M.; Burkholder, J.M. Harmful algal blooms and eutrophication: Nutrient sources, composition, and consequences. *Estuaries* **2002**, *25*, 704–726. [CrossRef]
9. Norris, G.; Mcandrews, J.H. Dinoflagellate cysts from post-glacial lake muds, Minnesota (USA). *Rev. Paleobot. Palynol.* **1970**, *10*, 131–156. [CrossRef]
10. Thiel, T.; Wolk, C.P. Metabolic activities of isolated akinetes of the cyanobacterium Nostoc spongiaeforme. *J. Bacteriol. Res.* **1983**, *156*, 369–374. [CrossRef]
11. Moore, D.; O'Donohue, M.; Garnett, C.; Critchley, C.; Shaw, G. Factors affecting akinete differentiation in *Cylindrospermopsis raciborskii* (Nostocales, Cyanobacteria). *Freshw. Biol.* **2005**, *50*, 345–352. [CrossRef]
12. Sukenik, A.; Kaplan-Levi, R.N.; Viner-Mozzini, Y.; Lupu, A.; Sela, D. Induction, Isolation and Counting of Akinetes in *Aphanizomenon ovalisporum*. *Bio-protoc* **2016**, *6*, e1808. [CrossRef]
13. Kwon, D.; Kim, K.; Jo, H.; Lee, S.D.; Yun, S.M.; Park, C. Environmental factors affecting akinete germination and resting cell awakening of two cyanobacteria. *Appl. Microsc.* **2023**, *53*, 1–13. [CrossRef]
14. Legrand, B.; Miras, Y.; Beauger, A.; Dussauze, M.; Latour, D. Akinetes and ancient DNA reveal toxic cyanobacterial recurrences and their potential for resurrection in a 6700-year-old core from a eutrophic lake. *Sci. Total Environ.* **2019**, *687*, 1369–1380. [CrossRef]
15. Kang, Y.-J.; Moon, C.-H.; Cho, H.-J. Comparison of panning and sodium polytungstate methods for separating dinoflagellate cysts. *J. Fish Aquat. Sci.* **2008**, *41*, 228–231. [CrossRef]
16. Kang, Y.J. *Distribution of Dinoflagellate Cyst and Germination Using SPT Solution in Eutrophic Region of Southern Coastal Waters of Korea*; Pukyong National University: Busan, Republic of Korea, 2007.
17. D'agostino, P.M.; Woodhouse, J.N.; Makower, A.K.; Yeung, A.C.; Ongley, S.E.; Micallef, M.L.; Moffitt, M.C.; Neilan, B.A. Advances in genomics, transcriptomics and proteomics of toxin-producing cyanobacteria. *Environ. Microbiol. Rep.* **2016**, *8*, 3–13. [CrossRef]
18. Liu, Y.; Ren, Z.; Qu, X.; Zhang, M.; Yu, Y.; Zhang, Y.; Peng, W. Microbial community structure and functional properties in permanently and seasonally flooded areas in Poyang Lake. *Sci. Rep.* **2020**, *10*, 1–11.
19. Rasmussen, J.P.; Monis, P.T.; Saint, C.P. *Early Detection of Cyanobacterial Toxins Using Genetic Methods*; American Water Works Association Research Foundation: Denver, CO, USA, 2008.
20. Tsao, H.-W.; Michinaka, A.; Yen, H.-K.; Giglio, S.; Hobson, P.; Monis, P.; Lin, T.-F. Monitoring of geosmin producing *Anabaena circinalis* using quantitative PCR. *Water Res.* **2014**, *49*, 416–425. [CrossRef]
21. Ueno, Y.; Nagata, S.; Tsutsumi, T.; Hasegawa, A.; Watanabe, M.F.; Park, H.-D.; Chen, G.-C.; Chen, G.; Yu, S.-Z. Detection of microcystins, a blue-green algal hepatotoxin, in drinking water sampled in Haimen and Fusui, endemic areas of primary liver cancer in China, by highly sensitive immunoassay. *Carcinogs* **1996**, *17*, 1317–1321. [CrossRef]
22. Vaitomaa, J.; Rantala, A.; Halinen, K.; Rouhiainen, L.; Tallberg, P.; Mokelke, L.; Sivonen, K. Quantitative real-time PCR for determination of microcystin synthetase E copy numbers for *Microcystis* and *Anabaena* in lakes. *Appl. Environ. Microbiol.* **2003**, *69*, 7289–7297. [CrossRef]
23. Ramm, J.; Lupu, A.; Hadas, O.; Ballot, A.; Rücker, J.; Wiedner, C.; Sukenik, A. A CARD-FISH protocol for the identification and enumeration of cyanobacterial akinetes in lake sediments. *FEMS Microbiol. Ecol.* **2012**, *82*, 23–36. [CrossRef]
24. Wootton, J.C.; Federhen, S. Statistics of local complexity in amino acid sequences and sequence databases. *Comput. Chem.* **1993**, *17*, 149–163. [CrossRef]
25. Kodama, Y.; Shumway, M.; Leinonen, R. The Sequence Read Archive: Explosive growth of sequencing data. *Nucleic Acids Res.* **2011**, *40*, D54–D56. [CrossRef]
26. Park, Y.M.; Squizzato, S.; Buso, N.; Gur, T.; Lopez, R. The EBI search engine: EBI search as a service—Making biological data accessible for all. *Nucleic Acids Res.* **2017**, *45*, W545–W549. [CrossRef]
27. Li, X.; Dreher, T.W.; Li, R. An overview of diversity, occurrence, genetics and toxin production of bloom-forming *Dolichospermum* (*Anabaena*) species. *Harmful Algae* **2016**, *54*, 54–68. [CrossRef]
28. Stein, J.R. *Handbook of Phycological Methods: Culture Methods and Growth Measurements*; CUP archive; Cambridge University Press: Cambridge, UK, 1979; Volume 1.
29. Stanier, R.Y.; Kunisawa, R.; Mandel, M.; Cohen-Bazire, G. Purification and properties of unicellular blue-green algae (order Chroococcales). *Bacteriol. Rev.* **1971**, *35*, 171. [CrossRef]
30. Park, C.-H.; Park, M.-H.; Kim, K.H.; Park, J.-H.; Kwon, D.-R.; Kim, N.Y.; Lim, B.-J.; Hwang, S.-J. Akinete germination chamber: An experimental device for cyanobacterial akinete germination and plankton emergence. *Harmful Algae* **2018**, *72*, 74–81. [CrossRef]
31. Egeler, P.; Römbke, J.; Meller, M.; Knacker, T.; Nagel, R. Bioaccumulation test with Tubificid Sludgeworms in artificial media–development of a standardisable method. *Hydrobiologia* **1999**, *406*, 271–280. [CrossRef]
32. Li, R.; Watanabe, M.; Watanabe, M.M. Taxonomic studies of planktic species of *Anabaena* based on morphological characteristics in cultured strains. *Hydrobiologia* **2000**, *438*, 117–138. [CrossRef]

33. Park, C.H. *Study on the Akinete Life Cycle and Vegetative Cell Dynamics in a Harmful Cyanobacterium, Dolichospermum circinale (Nostocales)*; Konkuk University: Seoul, Republic of Korea, 2018.
34. Guillard, R.R. Culture of phytoplankton for feeding marine invertebrates. In *Culture of Marine Invertebrate Animals*; Springer: Berlin/Heidelberg, Germany, 1975; pp. 29–60.
35. Kruger, N.J. The Bradford method for protein quantitation. In *The Protein Protocols Handbook*; Springer: Berlin/Heidelberg, Germany, 2009; pp. 17–24.
36. Shevchenko, A.; Tomas, H.; Havli, J.; Olsen, J.V.; Mann, M. In-gel digestion for mass spectrometric characterization of proteins and proteomes. *Nat. Protoc.* **2006**, *1*, 2856. [CrossRef]
37. Maier, T.; Kostrzewa, M. Fast and reliable MALDI-TOF MS-based microorganism identification. *Chim. Oggi* **2007**, *25*, 68. [CrossRef]
38. O'Leary, N.A.; Wright, M.W.; Brister, J.R.; Ciufo, S.; Haddad, D.; McVeigh, R.; Rajput, B.; Robbertse, B.; Smith-White, B.; Ako-Adjei, D. Reference sequence (RefSeq) database at NCBI: Current status, taxonomic expansion, and functional annotation. *Nucleic Acids Res.* **2015**, *44*, D733–D745. [CrossRef]
39. Tatusova, T.; DiCuccio, M.; Badretdin, A.; Chetvernin, V.; Nawrocki, E.P.; Zaslavsky, L.; Lomsadze, A.; Pruitt, K.D.; Borodovsky, M.; Ostell, J. NCBI prokaryotic genome annotation pipeline. *Nucleic Acids Res.* **2016**, *44*, 6614–6624. [CrossRef]
40. Brister, J.R.; Ako-Adjei, D.; Bao, Y.; Blinkova, O. NCBI viral genomes resource. *Nucleic Acids Res.* **2014**, *43*, D571–D577. [CrossRef]
41. Pisitkun, T.; Hoffert, J.D.; Saeed, F.; Knepper, M.A. NHLBI-AbDesigner: An online tool for design of peptide-directed antibodies. *Am. J. Physiol. Cell Physiol.* **2011**, *302*, C154–C164. [CrossRef]
42. Cardemil, L.; Wolk, C.P. The polysaccharides from heterocyst and spore envelopes of a blue-green alga. Methylation analysis and structure of the backbones. *Biol. Chem.* **1976**, *251*, 2967–2975. [CrossRef]
43. Cardemil, L.; Wolk, C.P. Polysaccharides from the envelopes of heterocysts and spores of the blue-green algae *Anabaena variabilis* and *Cylindrospermum licheniforme*. *J. Phycol.* **1981**, *17*, 234–240. [CrossRef]
44. Graham, L.E.; Wilcox, L.W. *Algae*; Prentice Hall: Upper Saddler River, NJ, USA, 2000; Volume 25, p. 29.
45. Maheshwari, R.; Bharadwaj, G.; Bhat, M.K. Thermophilic fungi: Their physiology and enzymes. *Microbiol. Mol. Biol. Rev.* **2000**, *64*, 461–488. [CrossRef]
46. Raugei, G.; Ramponi, G.; Chiarugi, P. Low molecular weight protein tyrosine phosphatases: Small, but smart. *Cell Mol. Life Sci.* **2002**, *59*, 941–949. [CrossRef]
47. da Silva Aires, R.; Steindorff, A.S.; Ramada, M.H.S.; de Siqueira, S.J.L.; Ulhoa, C.J. Biochemical characterization of a 27 kDa 1, 3-β-D-glucanase from *Trichoderma asperellum* induced by cell wall of Rhizoctonia solani. *Carbohydr. Polym.* **2012**, *87*, 1219–1223. [CrossRef]
48. Zhou, R.; Wolk, C.P. Identification of an akinete marker gene in *Anabaena variabilis*. *J. Bacteriol. Res.* **2002**, *184*, 2529–2532. [CrossRef]
49. Qiu, Y.; Gu, L.; Brözel, V.; Whitten, D.; Hildreth, M.; Zhou, R. Unique proteomes implicate functional specialization across heterocysts, akinetes, and vegetative cells in *Anabaena cylindrica*. *bioRxiv* **2020**. [CrossRef]
50. Bryant, D.A. *The Molecular Biology of Cyanobacteria*; Springer Science & Business Media: Berlin/Heidelberg, Germany, 2006; Volume 1.
51. Flores, F.G. *The Cyanobacteria: Molecular Biology, Genomics, and Evolution*; Horizon Scientific Press: Poole, UK, 2008.
52. Perez, R.; Forchhammer, K.; Salerno, G.; Maldener, I. Clear differences in metabolic and morphological adaptations of akinetes of two Nostocales living in different habitats. *Microbiology* **2016**, *162*, 214–223. [CrossRef]
53. Singh, H.; Sunita, K. A biochemical study of spore germination in the blue-green alga *Anabaena doliolum*. *J. Exp. Bot.* **1974**, *25*, 837–845. [CrossRef]
54. Zheng, L.; Donovan, W.P.; Fitz-James, P.C.; Losick, R. Gene encoding a morphogenic protein required in the assembly of the outer coat of the Bacillus subtilis endospore. *Genes Dev.* **1988**, *2*, 1047–1054. [CrossRef]
55. Abhyankar, W.; de Koning, L.J.; Brul, S.; de Koster, C.G. Spore proteomics: The past, present and the future. *FEMS Microbiol. Lett.* **2014**, *358*, 137–144. [CrossRef]
56. Setlow, B.; Hand, A.; Setlow, P. Synthesis of a Bacillus subtilis small, acid-soluble spore protein in Escherichia coli causes cell DNA to assume some characteristics of spore DNA. *J. Bacteriol.* **1991**, *173*, 1642–1653. [CrossRef]
57. Zhang, G.; An, Y.; Zabed, H.M.; Guo, Q.; Yang, M.; Yuan, J.; Li, W.; Sun, W.; Qi, X. Bacillus subtilis Spore Surface Display Technology: A Review of Its Development and Applications. *J. Microbiol. Biotechnol.* **2019**, *29*, 179–190.
58. Abel-Santos, E. Endospores, sporulation and germination. In *Molecular Medical Microbiology*; Elsevier: Amsterdam, The Netherlands, 2015; pp. 163–178.
59. Ow, S.Y.; Cardona, T.; Taton, A.; Magnuson, A.; Lindblad, P.; Stensjö, K.; Wright, P.C. Quantitative shotgun proteomics of enriched heterocysts from Nostoc sp. PCC 7120 using 8-plex isobaric peptide tags. *J. Proteome Res.* **2008**, *7*, 1615–1628. [CrossRef]
60. Brandão-Dias, P.F.; Rosi, E.J.; Shogren, A.J.; Tank, J.L.; Fischer, D.T.; Egan, S.P. Fate of environmental proteins (eProteins) from genetically Engineered crops in Streams is controlled by Water pH and ecosystem metabolism. *Environ. Sci.Technol.* **2021**, *55*, 4688–4697. [CrossRef]
61. Pandey, S.; Rai, R.; Rai, L.C. Proteomics combines morphological, physiological and biochemical attributes to unravel the survival strategy of *Anabaena* sp. PCC7120 under arsenic stress. *J. Proteom.* **2012**, *75*, 921–937. [CrossRef]

62. Panda, B.; Basu, B.; Rajaram, H.; Kumar Apte, S. Methyl viologen responsive proteome dynamics of *Anabaena* sp. strain PCC7120. *Proteomics* **2014**, *14*, 1895–1904. [CrossRef]
63. Battchikova, N.; Muth-Pawlak, D.; Aro, E.-M. Proteomics of cyanobacteria: Current horizons. *Curr. Opin. Biotechnol.* **2018**, *54*, 65–71. [CrossRef]
64. Sound, J.K.; Bellamy-Carter, J.; Leney, A.C. The increasing role of structural proteomics in cyanobacteria. *Essays Biochem.* **2023**, *67*, 269–282.